ACS Photonics

Article

pubs.acs.org/journal/apchd5

Disorder as a Playground for the Coexistence of Optical Nonlinear Effects: Competition between Random Lasing and Stimulated Raman Scattering in Complex Porous Materials

Nicolas Bachelard,[†] Preeti Gaikwad,[‡] Rénal Backov,[‡] Patrick Sebbah,[†] and Renaud A. L. Vallée*[,‡]

[†]Institut Langevin, ESPCI ParisTech, CNRS, 1 Rue Jussieu, 75238 Paris Cedex 05, France

[‡]CNRS, University Bordeaux, CRPP, UPR 8641, 115 Avenue Schweitzer, 33600 Pessac, France

ABSTRACT: We predict the coexistence and competition of random lasing and stimulated Raman scattering (SRS) in active disordered random media. We develop a simple model that includes both mechanisms coupled to diffusion equation. We find that the prevalence of a nonlinear mechanism over the other is determined by the degree of scattering. This is confirmed experimentally in dye-infiltrated three-dimensional porous silica-based disordered samples, with controllable pore size and transport properties. Experimentally, random lasing dominates in a sample with a large transport mean free path, $l_t \approx 100$ μm, while it gives way to SRS for $l_t \approx 25$ μm. The competition is explained in terms of disorder-dependent pump depletion and fluorescence saturation.

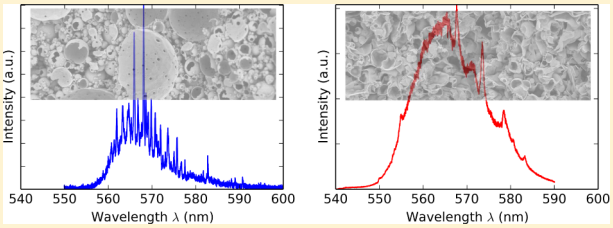

KEYWORDS: *random lasers, Raman lasers, nonlinear effects, porous materials*

Competition between different nonlinear phenomena in a single medium is still a pristine domain of investigation. The quenching of a resonant optical nonlinearity in physical situations where a competition exists with a parametric process has been demonstrated to be a general feature of nonlinear optics.[1,2] The parametric suppression of stimulated Raman scattering (SRS) has been predicted by Bloembergen and Shen[3,4] and observed experimentally;[5] the suppression of multiphoton ionization by third-harmonic generation[6,7] and the suppression of amplified spontaneous emission by four-wave mixing pumped by two-photon excitation[8,9] are two other systems exhibiting similar behaviors.

Besides these initially largely unexpected results, other nonlinear interactions have been shown to play an important role in lasers. A Kerr nonlinearity changes the frequency and quality factor of a defect mode. The dynamic effect of a Kerr nonlinearity on the spatial size and intensity of a weakly disordered photonic crystal defect[10]/random medium[11] lasing mode has been reported. The spatial and temporal characteristics of filamentation in broad-area semiconductor lasers have been theoretically[12] and experimentally[13] investigated. The dynamics of feedback-induced instability and chaos in semiconductor lasers and their applications have been reviewed.[14] More recently, the competition between stimulated Brillouin scattering (SBS) and SRS in gases has been shown to depend on pressure and the focusing optics.[15,16]

The presence of SRS in laser amplification is an important example of the coexistence and interaction of nonlinear effects.[17] Besides, SRS is known to be a significant limitation to pulse propagation in long-distance fibers,[18−20] and various techniques (e.g., chirp pulse amplification[21]) have been proposed to hinder its impact on amplification.

The interaction of light with a medium at frequencies near the electronic resonance of an atomic or molecular transition involves phenomena such as absorption, stimulated and spontaneous emission. These interactions become nonlinear when the light is sufficiently intense so that the populations of the various energy levels are significantly altered. Since the pioneering work of Letokhov[22] predicting light amplification through stimulated emission in open disordered active media, random lasers have raised increasing interest.[23−26] Here, the optical cavity of conventional lasers is replaced by an open scattering medium to provide optical feedback. Multiple scattering increases the effective optical path length within the gain medium and offers a unique degree of freedom to tune or control light−matter interaction. Emission spectrum[27,28] and laser directivity,[29] mode competition,[28] and laser coherence[30] are examples of laser characteristics that can be manipulated, a versatility not readily available in regular lasers.

Multiple scattering may also enhance other optical nonlinear interactions in disordered media, such as the Kerr effect,[31] four-wave mixing,[32] or Raman gain,[33−36] to mention a few. The picture may become extremely complex when such effects start to compete with each other. SRS is characterized by the stimulated conversion of photons from an intense optical pump wave into lower frequency Stokes photons through the resonant excitation of a vibration in the transmission medium. The resonant nature of SRS is due to the fact that the beating frequency between the pump and the Stokes wave matches a vibrational transition of the medium.[37] By introducing the

Received: August 1, 2014
Published: October 14, 2014

optical pump wave depletion through SRS, Shen and Bloembergen[4] obtained a qualitative description of wave interaction and saturation effects in a homogeneous system. In a scattering medium where nonlinear interaction is enhanced, the question is raised whether random lasing (RL) is the dominant mechanism or the pump beam could be preferentially converted into a Stokes (SRS) beam and random lasing superseded, as Raman transitions are much faster than electronic transitions.

In this article, we illustrate how disordered systems may offer an interesting platform to explore the interaction between different nonlinear optical effects. In particular, we investigate the competition between RL and SRS in random media with gain and show that, by changing the degree of scattering, one may tune the interaction length to activate, bring to coexistence, or suppress these nonlinear mechanisms.

By coupling the diffusion equation to the rate equations of a four-level system and to the Raman rate equation, we show that (a) the scattering strength of the disordered system provides a new degree of freedom to tune the light−matter interaction length, able to activate or suppress nonlinear mechanisms, and (b) the pump depletion is a key ingredient to capture the physics of the transition from RL to SRS and to predict the experimental parameters required for their simultaneous observation. Our model reveals that SRS occurs in strongly scattering random lasers with a small mean free path, while RL dominates in weakly scattering samples with a larger transport mean free path. This prediction is confirmed experimentally: We report on the observation of both random lasing and SRS in dye-infiltrated porous scattering silica-based samples. Using a controlled fabrication process, scattering samples are designed with various transport characteristics to explore the role of multiple scattering in the competition between RL and SRS. We anticipate that our model can easily be extended to other nonlinear mechanisms and represents an interesting tool in the exploration of nonlinear light−matter interaction in complex media.

EXPERIMENTAL SECTION

Synthetic procedures are based on the use of both micelles and direct concentrated emulsion templates.[38] Typically 5.7 g of tetraethoxyorthosilane (TEOS) is added to 16.5 g of tetradecyltrimethylammonium bromide (TTAB) aqueous solution at 35% in weight. The aqueous mixture is then brought to a pH value close to 0 (6.7 mL of HCl 37%), leading, after the oil emulsification process, washing, and thermal treatment, to the materials labeled Si(HIPE) (silica-based high internal phase emulsion). We have performed the syntheses of two Si(HIPE) foams emerging from the use of starting concentrated direct emulsion at two oil volume fractions (f_v) where 35 g (f_v = 0.67) and 60 g (f_v = 0.78) of dodecane are respectively emulsified. In the following the corresponding macrocellular foams are labeled 35-Si(HIPE) and 60-Si(HIPE). SEM observations are performed with a Jeol JSM-840A scanning electron microscope operating at 10 kV. The specimens are gold-coated or carbon-coated prior to examination.

We use a white light illumination lamp (fiber-coupled white light HL-2000-HP-FHSA, Ocean Optics) combined with an integrating sphere (fiber-coupled integrating sphere FOIS-1, Ocean Optics) and a spectrometer (fiber spectrometer USB2000+VIS-NIR, Ocean Optics) to measure the total integrated forward scattering $T(L)$ versus sample thickness L ranging from less than 1 to more than 10 mm, for the two types of samples.

The second harmonic (λ_p = 532 nm) of a mode-locked Nd:Yag/YVO laser (τ_p = 28 ps pulsewidth, from Ekspla) is used to pump the Si(HIPE) at a 1 Hz repetition rate. The pump beam is focalized on a 200 μm diameter spot by an f = 23 mm lens. Scattered light is collected in reflection via an optical fiber connected to a Horiba iHR550 imaging spectrometer equipped with a 2400 mm^{-1} grating and a liquid nitrogen-cooled Symphony II camera (sampling rate 1 MHz, 1024 × 56 pixels, 26 μm pixel pitch). The entrance slit is 50 μm. The resulting spectral resolution is 20 pm. The integrating time is 1 s, and each spectrum is averaged 10 times.

RESULTS AND DISCUSSION

We consider a four-level laser system such as rhodamine 6G.[39] This system is pumped into an excited state $|2\rangle$, which decays rapidly to a metastable state $|1\rangle$. The laser transition occurs from this metastable state to a state $|0'\rangle$ just above the ground state, which decays rapidly to the actual ground state $|0\rangle$. This means that states $|2\rangle$ and $|0'\rangle$ are nearly unpopulated and that the population of state $|1\rangle$ can be described by one rate equation. This system is very close to the one used in Wiersma et al.[40] to model random lasing solely. Following Shen et al.,[4] we add a Raman radiation contribution that directly originates from the pump field. Because the transport mean free path is much smaller than the system size, we apply the diffusion approximation and assume that intensity is scattered uniformly in all directions. Diffusion equations can be reduced to 1D along the direction of the incident pump pulse, as in ref 40. The complete set of coupled differential equations describing our system is formed by three diffusion equations for pump, RL, and SRS photon densities, n_P, n_{RL}, and n_{SRS}, respectively, in addition to the rate equation for the density of dye molecules in state $|1\rangle$, $N_1(r, t)$:

$$\frac{\partial n_P}{\partial t} = D\nabla^2 n_P - \sigma_{abs} v(N_{tot} - N_1)n_P + \frac{I_{coll}(z, t)}{Sl_t hc/\lambda_p \tau_p} - g_r n_{SRS} n_P - \sigma_R v(N_{tot} - N_1)n_P \quad (1)$$

$$\frac{\partial n_{RL}}{\partial t} = D\nabla^2 n_{RL} + \sigma_{em} v N_1 n_{RL} + \frac{1}{\tau_e} N_1 \quad (2)$$

$$\frac{\partial n_{SRS}}{\partial t} = D\nabla^2 n_{SRS} + g_r n_P n_{SRS} + \sigma_R v(N_{tot} - N_1)n_P \quad (3)$$

$$\frac{\partial N_1}{\partial t} = \sigma_{abs} v(N_{tot} - N_1)n_P - \sigma_{em} v N_1 n_{RL} - \frac{1}{\tau_e} N_1 \quad (4)$$

where c is the speed of light in a vacuum, h is Planck's constant, $v = c/n_s$ is the celerity, l_t is the transport mean free path, and $D = vl_t/3$ is the diffusion coefficient of the light wave in the disordered medium. τ_e = 3.7 ns,[39] σ_{abs} = 3.8 × 10^{-16} cm^2,[39] σ_{em} = 1.2 × 10^{-16} cm^2,[39] $\sigma_R \simeq$ 2.0 × 10^{23} cm^2/molecule,[41] and $g_r = (2N\lambda_s^3/hcn_s^2\Gamma)(\partial\sigma/\partial\Omega)$[42] are the R6G spontaneous decay time, absorption cross-section, emission cross-section, Raman scattering cross-section, and Raman gain coefficient, respectively. In g_r, n_s = 1.05 and λ_s are the refractive index and wavelength at the Stokes frequency (taken to be the same as the excitation frequency, $\lambda_s = \lambda_p$, for the sake of simplicity in the model). N = 4.5 × 10^{18} cm^{-3} is the R6G density and Γ the width of the Raman line with $1/\Gamma$ = 5 × 10^{-12} s.

dx.doi.org/10.1021/ph500280m | ACS Photonics 2014, 1, 1206−1211

$I_{coll}(z, t)$ is the fluence of the incoming pump pulse, which, according to our experimental setup, is chosen to be a pulse centered on λ_p = 530 nm with a τ_p = 30 ps fwhm focused on a focal spot of 200 μm diameter, fixing the size area S of the incoming beam.

$$I_{coll}(z, t) = I_{in}\sqrt{\frac{b}{\pi}}\, e^{-z/l_t} e^{-b(t-t_p-z/v)^2/\tau_p^2} \quad (5)$$

where $b = 4\ln(2)$ and t_p is the time at which the maximum of the incident pulse hits the sample surface.

This simple model presents a strong simplification of the physics involved in complex three-dimensional (3D) systems, like the one considered hereafter. Such a model, which ignores the wave nature of light both in the rate equations and in the diffusion equation, cannot for instance predict the wavelength of the lasing modes. However, its version without SRS has been tested successfully in the past to study random lasing.[40] By including the rate equation for SRS, we show in this work that it captures the essential mechanisms involved and provides qualitative predictions that agree with experimental observations. The model does not intend to provide a quantitative description of the physics but to be simple and tractable numerically. In particular, coherence and interference effects are neglected. Nevertheless, this incoherent description allows the computation of physical parameters (e.g., threshold values) that consistently describe the competition mechanism between SRS and RL.

For simplicity, we use the same value of the diffusion constant for the pump, SRS, and RL, although different values could easily be incorporated. The first right-hand term of eqs 1−3 describes standard diffusion. The second term of eq 1 represents absorption of diffuse pump light, while the fourth and fifth terms represent the nonlinear coupling between the pump and Raman fields and the spontaneous Raman scattering term, properly counterbalanced by the second and third term in eq 3, respectively. The third term in eq 3 represents the scattering of the coherent pump pulse. The third term in eq 4 represents spontaneous emission.

We solve the set of eqs 1−5 numerically using the standard forward Euler discretization for the time derivative and second-order space derivative. In order to fully satisfy the diffusion approximation $\lambda < l_t \ll L$, we have chosen a transport mean path l_t ranging from 1 to 500 μm, while fixing $L = 100\ l_t$ (along the z coordinate axis used in eqs 1−5). By increasing the pump fluence I_{in} in a stepwise manner, we found a dissimilar dynamical behavior for small and large l_t. Figure 1 illustrates these differences. In the case of a large mean free path l_t = 500 μm, random lasing (black dotted curve) is first triggered at a threshold of ∼3 μJ (Figure 1c). The depletion of the excited state (red dotted curve) occurs simultaneously with the buildup of the RL pulse (Figure 1a). At larger pump fluence, SRS emerges (18 μJ) and eventually overcomes RL (34.5 μJ), the latter experiencing saturation (Figure 1c). Well contrasted with this situation is the case of stronger scattering corresponding to a small l_t = 1 μm (Figure 1b and d), where SRS (green dashed curve) directly dominates the response at low pump fluence, while RL is inhibited. The threshold for Raman in this case is found to be 3 μJ.

These calculations reveal the coexistence of RL and SRS in scattering samples under particular conditions of scattering and focused light on the specific mechanisms at work. For RL to be triggered, population inversion is required to populate the first

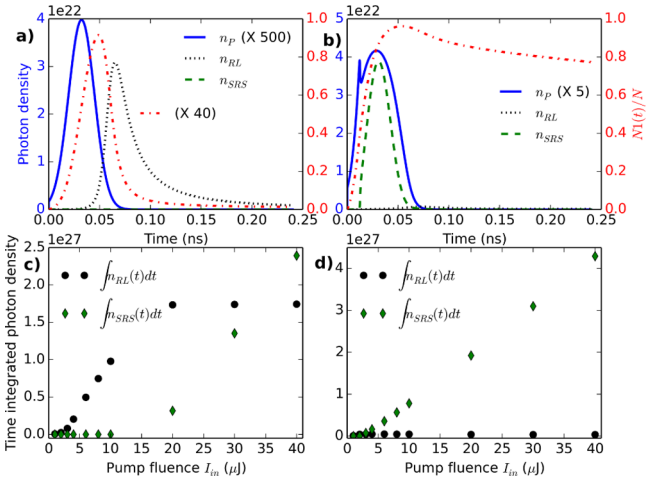

Figure 1. (a, b) Temporal profiles of n_P, n_{RL}, and n_{SRS}, the photon densities of the pump, RL, and SRS processes at low pump fluence (10 μJ for both), and (c, d) their time-integrated characteristics computed from eqs 1−5 in backscattering geometry for disordered systems with (a, c) l_t = 500 μm and (b, d) l_t = 1 μm. The initial pump pulse duration (blue solid line) is 30 ps. The red dashed-dotted line shows the time-dependent evolution of the population in the excited level, N_1/N_t. (c, d) Green diamonds (black dots) represent the time-integrated SRS (RL) photon density for increasing pump fluence I_{in}.

excitation level. It is the depletion of this level that leads to the emergence of RL (Figure 1a). In contrast, the SRS maximum energy density, n_{SRS}, directly emerges from the depletion of the pump energy density (Figure 1b). Since the Raman process is extremely fast, once the Raman threshold is reached, the pump energy density is rapidly converted into SRS. Population inversion N_1, which occurs on a longer time scale, is strongly impeded, resulting either in the saturation (Figure 1c) or the preclusion (Figure 1d) of the RL. Therefore, at large enough pump fluence, SRS is always the dominant radiation mechanism. Actually, the concomitance of the RL saturation with the onset of SRS seen in Figure 1c is not accidental: It is confirmed in Figure 2a, where the dependence on the mean free path of the SRS threshold I_{SRS} (green diamond) and the pump intensity at which RL saturates I_S (open squares) are found to overlap. This is a clear signature of the competition at work between electronic transition-based RL and vibrational transition-based SRS in disordered media.[37]

It is important to note here that, while the RL threshold I_{RL} is expected to be independent of l_t in the framework of our model, as a CW regime analysis already showed for a "pure" random laser operating in the diffusion approximation regime,[22,43−45] the latter regulates the SRS threshold, I_{SRS}, and, consequently, the pump fluence I_{RL-SRS} at which the SRS and RL responses cross. This is demonstrated in Figure 2a, where I_{RL}, I_{SRS}, and I_{RL-SRS} have been computed for increasing value of the mean free path. Increasing scattering strength increases the nonlinear interaction length and, as a result, favors Raman amplification. In contrast, RL is left unchanged. Although SRS always sets in at larger threshold values compared to RL (Figure 2a), it is nevertheless possible to observe Raman lasing, provided that the crossing between the two mechanisms (RL and SRS) occurs at low pump fluence. At l_t = 1 μm, $I_{FR} \approx 3$ μJ (Figure 2a) and SRS dominates at reasonable pump fluence (Figure 1d).

Having determined the conditions for which either RL or SRS dominates the lasing emission, we are now in a position to

dx.doi.org/10.1021/ph500280m | ACS Photonics 2014, 1, 1206−1211

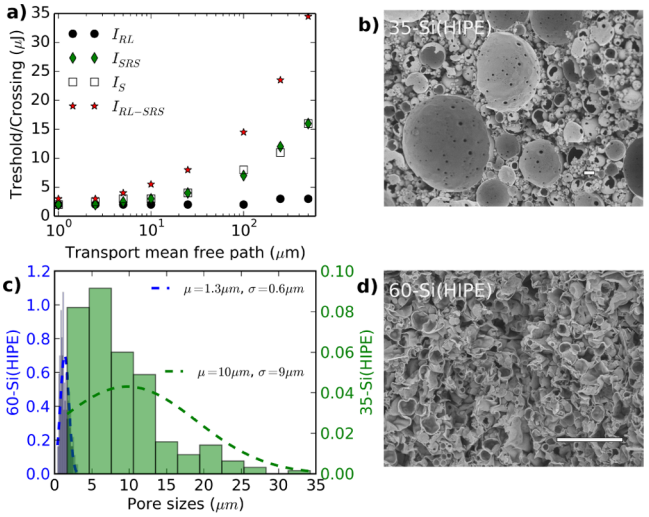

Figure 2. (a) Dependence on transport mean free path, l_t, of (black dots) RL threshold, I_{RL} (green diamonds), SRS thresholds, I_{SRS} (open squares), pump fluence at RL saturation, I_S, and (red stars) crossing fluence between RL and SRS responses, I_{RL-SRS}. SEM micrographs (the scale bar is 10 μm in both cases) of the 35-Si(HIPE) (b) and 60-Si(HIPE) (d), together with their normalized distributions (blue: 60-Si(HIPE); green: 35-Si(HIPE)) of pore diameters (c). The dashed lines shown in c correspond to the respective fitted normal distributions with values of the average and standard deviation indicated in the legend.

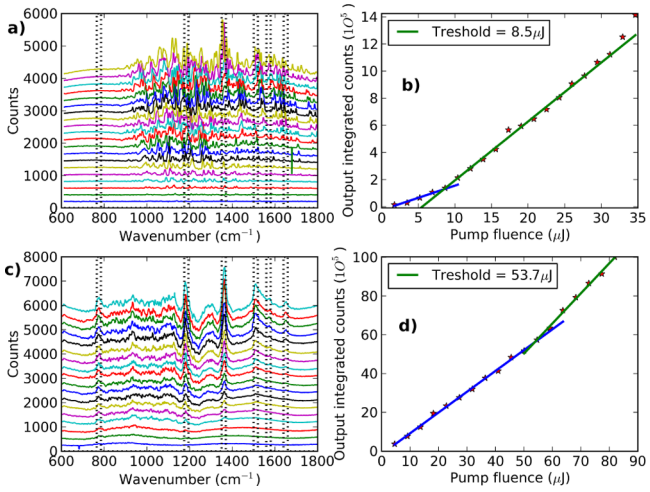

Figure 3. (a, c) Emission spectra with increasing pump fluence and (b, d) spectrally integrated laser characteristics for (a, b) large l_t = sample (35-Si(HIPE)) and (c, d) smaller l_t = sample (60-Si(HIPE)). In c, the dashed lines signal the Raman transitions of the RhB, also reported in a for comparison purposes.

engineer materials for which these two different lasing mechanisms might be observed. Let us note here that all numerical values used in the model are similar to available experimental structures. Rhodamine B (RhB) will be used experimentally as the gain medium instead of R6G, with very few changes in the spectroscopic properties.

From the material chemistry, as we increase the starting emulsion oil volume fraction, the macrocellular cell sizes diminish drastically and the size monodispersity of their distributions is reduced from 10 ± 9 μm (Figure 2b) to 1.3 ± 0.6 μm (Figure 2d) for 35-Si(HIPE) and 60-Si(HIPE), respectively, as shown by the normalized histograms and their fitted normal distributions in Figure 2c. As a consequence of the reduction of the macroporous void space diameters, l_t is expected to be smaller in the 60-Si(HIPE) than in the 35-Si(HIPE) structure.

The all-angle integrated forward scattering measurements are fitted with the stationary solution of the cylindrical diffusion equation including absorption,[46] which yields l_t and l_a. At 530 nm, l_t = 23 μm for the 60-Si(HIPE) and l_t = 100 μm for the 35-Si(HIPE). Their absorption length l_a is 1065 and 367 m, respectively. Such long l_a denote the negligible role of absorption in such structures, as clearly shown in ref 46.

Both samples are infiltrated under vacuum with a 10 μM ethanolic dye solution. The gain length l_g of the rhodamine B solution used is 138 μm. A thermogravimetric analysis gives the density of dye molecules infiltrated within the porous structures. We find $N_t = 1.87 \times 10^{25}/m^3$ in 60-Si(HIPE) and $9.03 \times 10^{24}/m^3$ in the 35-Si(HIPE).

Figure 3a and c show the spectra with increasing pump power for samples 35-Si(HIPE) and 60-Si(HIPE), respectively. These spectra have been median- and Fourier-filtered in order to remove the baseline. Spectra shown in Figure 3a bear the RL signatures with narrow peaks of ~2 cm^{-1} fwhm randomly distributed in the spectrum. This distribution is pump-position-dependent as expected in random lasing. Spectral drift of the lasing modes with pump power is characteristic of a third-order nonlinear gain effect. Spectra shown in Figure 3c are of a different nature. Broad peaks of ~5−10 cm^{-1} fwhm appearing at fixed and well-defined frequencies are identified as Raman resonances of the RhB: High-frequency peaks centered at 1185, 1360, 1510, 1570, and 1650 cm^{-1} (marked by dashed lines in Figure 3c) correspond to stretching modes of aromatic benzene rings, while the low-frequency peak centered at 775 cm^{-1} is associated with an out-of-plane bending motion of the hydrogen atoms of the xanthene skeleton.[47] We confirm that these peaks are independent of pump position and pump fluence. These two situations correspond to the extreme cases found theoretically where either RL lasing or SRS dominates, depending on the degree of scattering.

This is confirmed in Figure 3b and 3d, which show the lasing characteristics for the two samples. These measurements are reproduced for three different locations of the pump spot, yielding reproducible measurements of the lasing threshold. For the 35-Si(HIPE) sample, the RL threshold is 8.4, 8.4, and 8.5 μJ. Larger values are found for the SRS threshold of the 60-Si(HIPE) sample (60.1, 53.7, and 60.2 μJ). Higher pump fluence results in dye bleaching and sample damage, preventing the observation in 35-Si(HIPE) of the SRS emergence and its increase over RL, as predicted theoretically and shown in Figure 1c.

We point out that, based on considerations about resonant Raman scattering (RRS),[48] the appearance of SRS can be attributed neither to an electromagnetic enhancement effect, as there is no metal in the structures, nor to a chemical enhancement factor. Moreover, dye aggregation has been prevented by using a low concentration of RhB, and there is no structural difference between 35-Si(HIPE) and 60-Si(HIPE) that could cause a different fluorescence quenching or photobleaching of RhB that could explain the disappearance of RL.

dx.doi.org/10.1021/ph500280m | ACS Photonics 2014, 1, 1206−1211

CONCLUSION

We have predicted and observed experimentally the coexistence and competition of stimulated Raman scattering and random lasing in an optically pumped active disordered medium. We have shown that the interaction depends on its scattering strength. We have proposed a relatively simple model based on rate and diffusion equations, which revealed the role of multiple scattering in the balancing between SRS and RL. Experimentally, by properly engineering highly disordered porous samples with carefully designed distributions of pore sizes, we have been able to achieve structures of different scattering strengths. Random lasing has been shown to dominate in samples with a large transport mean free path, while strongly scattering samples favored SRS at reasonable pump fluence. It is worth noting that the nonlinear effects involved (SRS and RL) are mediated here by a single gain medium (rhodamine B), which provides both electronic and vibrational transitions. This is in contrast with earlier work in microdroplets,[49,50] where SRS and lasing resulted from the simultaneous pumping of two different media (ethanol and dye) and were therefore independent mechanisms.

In this work, we show that two nonlinear optical effects may coexist in a random media. We predict that similar coexistence could be obtained for other mechanisms (e.g., Kerr nonlinearity, stimulated Brillouin scattering). Remarkably, we demonstrate that the strength of the disorder provides us with the unique ability to trigger the interaction between both effects. Beyond the fundamental novelty of this work and the possibility to investigate and control nonlinear interactions, we anticipate a wealth of applications related to noninvasive biomedical imaging. In particular, recent papers have demonstrated the potential of SRS for biomedical imaging[51] and in vivo imaging,[52] by notably being able to probe molecular densities. In this work, we provide a complete description of the SRS's occurrence in random media. In particular, we determined how the transport mean free path regulated the SRS threshold. Accordingly, this feature could be used to probe the transport mean free path in biological tissue, by monitoring the threshold of the SRS emission.

AUTHOR INFORMATION

Corresponding Author

*E-mail: vallee@crpp-bordeaux.cnrs.fr.

Notes

The authors declare no competing financial interest.

ACKNOWLEDGMENTS

We acknowledge S. Bidault, C. Montes, R. Carminati, A. L. Burin, H. Cao, and J. P. Huignard for fruitful discussions. P.S. is grateful to the LABEX WIFI (Laboratory of Excellence within the French Program "Investments for the Future") under reference ANR-10-IDEX-0001-02 PSL* and the Groupement de Recherche 3219 MesoImage.

REFERENCES

(1) Wynne, J. Polarization renormalization due to nonlinear optical generation. *Phys. Rev. Lett.* **1984**, *52*, 751−754.
(2) Frey, R. Suppresion of the medium excitation in resonant nonlinear optics. *Opt. Commun.* **1992**, *89*, 441−446.
(3) Bloembergen, N.; Shen, Y. Coupling between vibrations and light waves in Raman laser media. *Phys. Rev. Lett.* **1964**, *12*, 504−507.
(4) Shen, Y. R.; Bloembergen, N. Theory of stimulated Brillouin and Raman scattering. *Phys. Rev.* **1965**, *137*, A1787−A1805.
(5) Golovchenko, E.; Mamyshev, P.; Pilipetskii, A.; Dianov, E. Mutual influence of the parametric effects and stimulated Raman scattering in optical fibers. *IEEE J. Quantum Electron.* **1990**, *26*, 1815−1820.
(6) Miller, J.; Compton, R.; Payne, M.; Garrett, W. Resonantly enhanced multiphoton ionization and third-harmonic generation in xenon gas. *Phys. Rev. Lett.* **1980**, *45*, 114−116.
(7) Glownia, J.; Sander, R. Experimental evidence for the competition between resonantly enhanced multiphoton ionization and third-harmonic generation in xenon. *Phys. Rev. Lett.* **1982**, *49*, 21−24.
(8) Malcuit, M.; Gauthier, D.; Boyd, R.; York, W. Suppression of amplified spontaneous emission by the four-wave mixing process. *Phys. Rev. Lett.* **1985**, *55*, 1086−1089.
(9) Boyd, R. W.; Malcuit, M.; Gauthier, D.; Rzaewski, K. Competition between amplified spontaneous emission and the four-wave-mixing process. *Phys. Rev. A* **1987**, *35*, 1648−1658.
(10) Liu, B.; Yamilov, A.; Cao, H. Effect of Kerr nonlinearity on defect lasing modes in weakly disordered photonic crystals. *Appl. Phys. Lett.* **2003**, *83*, 1092.
(11) Liu, B.; Yamilov, A.; Ling, Y.; Xu, J.; Cao, H. Dynamic nonlinear effect on lasing in a random medium. *Phys. Rev. Lett.* **2003**, *91*, 063903.
(12) Hess, O.; Koch, S. W.; Moloney, J. V. Filamentation and beam-propagation in broad-area semiconductor-lasers. *IEEE J. Quantum Electron.* **1995**, *31*, 35−43.
(13) Marciante, J. R.; Agrawal, G. P. Spatio-temporal characteristics of filamentation in broad-area semiconductor lasers: experimental results. *IEEE Photonics Technol. Lett.* **1998**, *10*, 54−56.
(14) Ohtsubo, J. Feedback induced instability and chaos in semiconductor lasers and their applications. *Opt. Rev.* **1999**, *6*, 1−15.
(15) Sentrayan, K.; Kushawaha, V. Competition between steady state stimulated Raman and Brillouin scattering processes in CH_4 and H_2. *J. Phys. D: Appl. Phys.* **1993**, *26*, 1554−1560.
(16) Yehud, L. B.; Belker, D.; Ravnitzki, G.; Ishaaya, A. Competition between stimulated Raman and Brillouin scattering processes in CF_4 gas. *Opt. Lett.* **2014**, *39*, 1026−9.
(17) Andryunas, K.; Vishchakas, Yu.; Kabelka, V.; Mochalov, I. V.; Pavlyuk, A. A. Stimulated-Raman self-conversion of Nd(3+) laser light in double tungstenate crystals. *JETP Lett.* **1985**, *42*, 410−412.
(18) Smith, R. G. Optical power handling capacity of low loss optical fibers as determined by stimulated Raman and brillouin scattering. *Appl. Opt.* **1972**, *11*, 2489−94.
(19) Dianov, E. M.; Karasik, A. Y.; Mamyshev, P. V.; Prokhorov, A. M.; Serkin, V. N.; Stel'makh, M. F.; Fomichev, A. A. Stimulated-Raman conversion of multisoliton pulses in quartz optical fibers. *JETP Lett.* **1985**, *41*, 242−244.
(20) Agrawal, G. P. Effect of gain dispersion and stimulated Raman scattering on soliton amplification in fiber amplifiers. *Opt. Lett.* **1991**, *16*, 226−8.
(21) Strickland, D.; Mourou, G. Compression of amplified chirped optical pulses. *Opt. Commun.* **1985**, *55*, 447−449.
(22) Letokhov, S. Generation of light by a scattering medium with negative resonance. *Sov. Phys. JETP* **1968**, *26*, 835−840.
(23) Cao, H. *Waves in Random Media*; Taylor & Francis, 2003; Vol. *13*, pp R1−R39.
(24) Wiersma, D. S. The physics and applications of random lasers. *Nat. Phys.* **2008**, *4*, 359−367.
(25) Wiersma, D. S.; Noginov, M. A. Nano and random lasers. *J. Opt.* **2010**, *12*, 020201.
(26) Wiersma, D. S. Disordered photonics. *Nat. Photonics* **2013**, *7*, 188−196.
(27) Bachelard, N.; Andreasen, J.; Gigan, S.; Sebbah, P. Taming random lasers through active spatial control of the pump. *Phys. Rev. Lett.* **2012**, *109*, 033903.
(28) Bachelard, N.; Gigan, S.; Noblin, X.; Sebbah, P. Adaptive pumping for spectral control of random lasers. *Nat. Phys.* **2014**, *10*, 426−431.

(29) Hisch, T.; Liertzer, M.; Pogany, D.; Mintert, F.; Rotter, S. Pump-controlled directional light emission from random lasers. *Phys. Rev. Lett.* **2013**, *111*, 023902.
(30) Redding, B.; Choma, M. A.; Cao, H. Speckle-free laser imaging using random laser illumination. *Nat. Photonics* **2012**, *6*, 355−359.
(31) Bortolozzo, U.; Residori, S.; Sebbah, P. Experimental observation of speckle instability in Kerr random media. *Phys. Rev. Lett.* **2011**, *106*, 103903.
(32) Guerin, W.; Michaud, F.; Kaiser, R. Mechanisms for lasing with cold atoms as the gain medium. *Phys. Rev. Lett.* **2008**, *101*, 093002.
(33) Turitsyn, S. K.; Babin, S. A.; El-Taher, A. E.; Harper, P.; Churkin, D. V.; Kablukov, S. I.; Ania-Castañón, J. D.; Karalekas, V.; Podivilov, E. V. Random distributed feedback fibre laser. *Nat. Photonics* **2010**, *4*, 231−235.
(34) Guerin, W.; Mercadier, N.; Brivio, D.; Kaiser, R. Threshold of a random laser based on Raman gain in cold atoms. *Opt. Express* **2009**, *17*, 11236−11245.
(35) Baudouin, Q.; Mercadier, N.; Guarrera, V.; Guerin, W.; Kaiser, R. A cold-atom random laser. *Nat. Phys.* **2013**, *9*, 357−360.
(36) Hokr, B. H.; Bixler, J. N.; Cone, M. T.; Mason, J. D.; Beier, H. T.; Noojin, G. D.; Petrov, G. I.; Golovan, L. a.; Thomas, R. J.; Rockwell, B. a.; Yakovlev, V. V. Bright emission from a random Raman laser. *Nat. Commun.* **2014**, *5*, 4356.
(37) Boyd, R. W. *Nonlinear Optics*, 3rd ed.; Academic Press, 2008.
(38) Carn, F.; Colin, A.; Achard, M.-F.; Deleuze, H.; Sellier, E.; Birot, M.; Backov, R. Inorganic monoliths hierarchically textured via concentrated direct emulsion and micellar templates. *J. Mater. Chem.* **2004**, *14*, 1370−1376.
(39) Duarte, F. J., Hillman, L. W., Eds. *Dye Laser Principles: With Applications (Google eBook)*; Elsevier, 2012.
(40) Wiersma, D. S.; Lagendijk, A. Light diffusion with gain and random lasers. *Phys. Rev. E* **1996**, *54*, 4256−4265.
(41) Shim, S.; Stuart, C. M.; Mathies, R. A. Resonance Raman cross-sections and vibronic analysis of rhodamine 6G from broadband stimulated Raman spectroscopy. *ChemPhysChem* **2008**, *9*, 697−699.
(42) Penzkofer, A.; Laubereau, A.; Kaiser, W. High intensity Raman interactions. *Prog. Quantum Electron.* **1979**, *6*, 55−140.
(43) Noginov, M. A.; Novak, J.; Williams, S. Modeling of photon density dynamics in random lasers. *Phys. Rev. A* **2004**, *70*, 063810.
(44) Noginov, M. A.; Fowlkes, I. N.; Zhu, G.; Novak, J. Random laser thresholds in cw and pulsed regimes. *Phys. Rev. A* **2004**, *70*, 043811.
(45) In some papers, the RL threshold depends on l_t, e.g., in ref 53. Thanks to a private communication with Professor Burin and co-workers, it turns out that, in their paper,[53] the absorption of the incident pump pulse by the gain medium is nonlinear (e.g., due to a strong pumping intensity). The resulting averaged absorbed pump density $I_p \propto I_0/(l_a l_t)^{1/2}$ (see eq 4), where I_0 stands for the external pump and l_a and l_t the absorption and transport mean free paths. In our model, the absorption is homogeneous along the system and reads $I_p \propto I_0(l_t/l_a)^{1/2}$. From this relation, one can demonstrate that the lasing threshold is independent from l_t as observed numerically, which is consistent with the prediction of Noginov[54] and another paper by Burin et al.[55]
(46) Gaikwad, P.; Ungureanu, S.; Backov, R.; Vynck, K.; Vallée, R. A. L. Photon transport in cylindrically-shaped disordered meso-macro-porous materials. *Opt. Express* **2014**, *22*, 7503−7513.
(47) Hildebrandt, P.; Stockburger, M. Surface-enhanced resonance Raman spectroscopy of rhodamine 6G adsorbed on colloidal silver. *J. Phys. Chem.* **1984**, *88*, 5935−5944.
(48) Ling, X.; Xie, L.; Fang, Y.; Xu, H.; Zhang, H.; Kong, J.; Dresselhaus, M. S.; Zhang, J.; Liu, Z. Can graphene be used as a substrate for Raman enhancement? *Nano Lett.* **2010**, *10*, 553−561.
(49) Latifi, H.; Biswas, A.; Armstrong, R. L.; Pinnick, R. G. Lasing and stimulated Raman scattering in spherical liquid droplets: time, irradiance, and wavelength dependence. *Appl. Opt.* **1990**, *29*, 5387−5392.
(50) Kwok, A. S.; Chang, R. K. Suppression of lasing by stimulated Raman scattering in microdroplets. *Opt. Lett.* **1993**, *18*, 1597.
(51) Freudiger, C. W.; Min, W.; Saar, B. G.; Lu, S.; Holtom, G. R.; He, C.; Tsai, J. C.; Kang, J. X.; Xie, X. S. Label-free biomedical imaging with high sensitivity by stimulated Raman scattering microscopy. *Science* **2008**, *322*, 1857−1861.
(52) Saar, B. G.; Freudiger, C. W.; Reichman, J.; Stanley, C. M.; Holtom, G. R.; Xie, X. S. Video-rate molecular imaging in vivo with stimulated Raman scattering. *Science* **2010**, *330*, 1368−1370.
(53) Ling, Y.; Cao, H.; Burin, A.; Ratner, M.; Liu, X.; Chang, R. Investigation of random lasers with resonant feedback. *Phys. Rev. A* **2001**, *64*, 063808.
(54) Noginov, M. *Solid-State Random Lasers*; Springer, 2005.
(55) Burin, A.; Ratner, M. Two-photon pumping of a random laser. *IEEE J. Sel. Top. Quantum Electron.* **2003**, *9*, 124−127.